Geofísica Internacional (2003), Vol. 42, Num. 4, pp. 575-587

Spatial variations of *b*-values in the subduction zone of Central America

David A. Monterroso and Ota Kulhánek
Department of Earth Sciences, Uppsala University, Sweden.

Received: August 28, 2002; accepted: April 29, 2003

RESUMEN

Estudiamos la distribución frecuencia-magnitud a lo largo de la trinchera mesoamericana (MAT), usando 2345 eventos del periodo 1964-1994. Utilizamos el catalogo regional MIDAS con magnitud de completitud de 4.2. Para mapear el valor *b* como función de la profundidad (enfoque unidimensional), aplicamos el procedimiento de ventanas deslizantes en la vertical. Cada ventana contiene un número constante de eventos. Para obtener más detalles en la distribución del valor *b*, proyectamos los hipocentros del catálogo en tres regiones (aproximadamente Guatemala-El Salvador, Nicaragua, Costa Rica), hacia planos perpendiculares a la trinchera. Luego, calculamos el valor *b* en volúmenes cilíndricos deslizantes (enfoque bidimensional) que contienen un número constante de eventos y con centros en los nodos de un enrejillado de 5 km x 5 km. El valor *b* varía significativamente a lo largo de la MAT. Identificamos valores altos de *b* en la parte superior de la litosfera subducida, a profundidades de 80-110 km por debajo de Guatemala y El Salvador, y a profundidades de 130-170 km por debajo de Nicaragua. Localizamos valores anómalos (altos) de *b* en la parte inferior de la litosfera, a profundidades de 50-90 km y 50-160 km por debajo de Guatemala-El Salvador y Nicaragua, respectivamente. Las anomalías observadas en la parte superior de la litosfera pueden estar relacionadas con deshidratación e incremento sucesivo de la presión de poro en la litosfera descendiente. Estos, a su vez, producirían el volcanismo que ocurre sobre las anomalías en la parte superior de la litosfera. Las anomalías en la parte inferior de la zona de Wadati-Benioff podrían estar asociadas con el alto gradiente térmico entre la litosfera y el manto.

PALABRAS CLAVE: Valor de *b*, zona de subducción, América Central, cadena volcánica, esfuerzo.

ABSTRACT

Frequency-magnitude distribution along the Mid-American Trench (MAT) has been studied by means of 2345 earthquakes during the period 1964-1994. We used the regional MIDAS catalogue with a magnitude of completeness of 4.2. To resolve the *b*-value as a function of depth (one dimensional approach), we applied vertically sliding windows containing a constant number of events. To obtain more details in the *b* distribution, we projected catalogue hypocenters in three selected regions (approximately Guatemala and El Salvador, Nicaragua, Costa Rica), onto planes perpendicular to the trench. The *b*-values were calculated in sliding cylindrical volumes (two-dimensional approach) containing a constant number of earthquakes and centered at nodes of a 5 km x 5 km grid. The *b*-value varies significantly along a large part of MAT. High *b*-values were identified in the upper part of the slab at depths of 80-110 km beneath Guatemala-El Salvador and at depths 130-170 km beneath Nicaragua. Anomalous (high) *b*-values in the lower part of the slab were located at depths of 50-90 km and 50-160 km beneath Guatemala-El Salvador and Nicaragua, respectively. Anomalies observed at the upper part of the slab may be related to dehydration and successive increase in pore pressure in the down-going lithosphere, which may generate volcanism above the anomalies in the upper part of the slab. Anomalies on the lower surface of the Wadati-Benioff zone are likely to be associated with high thermal gradients between the slab and mantle.

KEYWORDS: *b*-value, subduction zone, Central America, volcanic chain, stress.

INTRODUCTION

In the mid 1950's Gutenberg and Richter (1954) introduced a formula for the frequency magnitude earthquake distribution (FMD) $\log_{10}N = a\text{-}bM$, relating the cumulative (or absolute) number of events *"N"* with magnitude larger than *M*, to seismic activity *"a"* which depends upon the volume- and time-window considered and the size distribution *b*, i.e. the measure of the relative abundance of large to smaller shocks. *b* is a tectonic parameter that provides the possibility of describing the stress and/or material (structural) conditions in the focal region (Mogi 1962, Scholz 1968, Gibowicz 1974). High *b*-values are considered to be an indication of a low stress level in a seismogenetic zone (Scholz 1968, Wyss 1973). Increased material heterogeneity, or an increase in the thermal gradient, also results in high *b*-values (Mogi 1962, Warren and Latham 1970). Conversely, low *b* values are correlated with high stress conditions (Gibowitz, 1974). Since there are several possibilities, it may be difficult, without other clues, to propose correct cause-and-effect pairs for particular sets of anomalous *b*-value observations.

There still is some controversy among seismologists concerning the spatial and temporal variations of *b*. While some workers (Kagan 1999) suggest that *b* is essentially constant, others (Wiemer and Benoit 1996, Ayele and Kulhánek 1997, Wiemer *et al*. 1998, Gerstenberger *et al*. 2001) argue that significant spatial and temporal variations of *b*-value exist. Making use of selected available earthquake catalogues may reveal changes in *b*-values calculated to high significance levels. By varying the input parameters (e.g. window width, threshold magnitude, different earthquake catalogs) we may confirm that observed changes (anomalies) in *b*-values are stable and not a result of a given choice of input parameters.

Detailed studies of *b*-value distributions are important for several reasons. For instance, most of currently performed hazard investigations assume a constant *b*. It is obvious that space- and time-variable *b*-value will affect existing hazard maps. Also, anomalous (low) *b*-values are considered as potential long-term earthquake precursors, which could precede an impending strong shock (see e.g. Li Quan *et al*. 1978, Monterroso 1999). Wiemer and Benoit (1996), Wiemer *et al*. (1998) and Gerstenberger *et al*. (2001), among others, used the depth distribution of *b*-values to study structural anomalies and stress levels in the crust (identification of active magma bodies) as well as in the upper mantle (creation of a volcanic arc).

The issue addressed in this paper is the spatial variation of *b*-values in the Wadati-Benioff zone (WBZ), and beneath Central America along the Mid-American Trench (MAT) and to examine its possible correlation with source zones of regional volcanism. We use an earthquake catalogue which covers more than 30 years of observations, and we perform one- and two-dimensional high-resolution *b*-value mapping. Calculations are made in horizontal slices (one dimension) and along two vertical cross-sections (two dimensions), perpendicular to the trench for a depth range from 40 km (or 50 km) to about 200 km, to cover the source-region depth of arc volcanism (Gill 1981).

TECTONIC SETTING

In Central America, i.e. the isthmus between Guatemala and Panama and the adjacent areas, the tectonic pattern is controlled by interaction of four major plates, namely the Caribbean (CAR), Cocos (COC), Nazca (NAZ) and North America (NOA) plates as shown in Figure 1. To the south, the tectonic setting is complicated by the interaction of CAR with a smaller tectonic unit, called Panama block, and by the subduction of the Cocos Ridge, CR (Figure 1). South of Costa Rica, where CAR, COC and NAZ boundaries meet, there is a triple junction close to the area where CR encounters the Middle American Trench (Protti *et al*., 1994). COC descends beneath CAR and NOA along the trench with a relatively high speed, which varies from 72±3 mm/yr off coast of Guatemala to 102±5 mm/yr off coast of southern Costa Rica (Protti *et al*. 1994). There is a smooth change of the dip angle from about 33° beneath Guatemala to about 43° beneath Nicaragua. Direction of the volcanic chain axis changes from about N30°E to about N45°E roughly where the Fonseca gulf separates El Salvador and Nicaragua. Close to the Nicaragua-Costa Rica border there is a clear offset of the volcanic chain axis.

The seismicity of the isthmus is concentrated in the Pacific coastal regions (Figure 2). The arc volcanism in the region makes up the Central American Volcanic Chain consisting of several tens of active (e.g. Pacaya, Izalco, Cerro Negro, Arenal) and a number of extinct volcanoes. The chain follows the Pacific coast of the isthmus, roughly parallel to MAT. It extends from the Mexico-Guatemala border, where the chain intersects the CAR-NOA plate boundary (White, 1991), to central Costa Rica. As suggested by Guendel and Protti (1998) the sudden termination of the chain in the south is likely to be due to the subduction of a younger lithosphere. Due to different tectonic features along MAT and following roughly the division proposed recently by Guendel and Protti (1998), we divided the study area into three smaller units (A, B, C in Figure 2) and investigated each unit independently.

DATA AND METHODOLOGY

Calculations of *b*-values were carried out on the catalogue compiled through the sponsorship of the Pan-American Institute of Geography and History as reported by the Middle America Seismograph Consortium (MIDAS) agency. For more details the reader should consult Tanner and Shepherd (1997). The catalogue, referred to as MIDAS catalogue hereafter, comprises earthquake catalogues of Mexico, South America, Central America and the Caribbean prepared by four different agencies (UNAM, CERESIS, CEPREDENAC and UWI). It lists moment magnitudes and covers the time period from 1471 to the middle of 1994. The most reliable section of the catalogue covers only the more recent period from 1964 to 1994 (used in the present study), for which authors of the catalogue claim data completeness for $M \geq 4$. We consider the MIDAS catalogue to be the best data set currently available for the present study, due to its completeness, magnitude homogeneity and time window covered. To verify that the observed behavior of *b* is real and not caused merely by a selection of input data, we also examined the catalogue of Engdahl *et al*. (1998).

Since we attempt to extract and analyze events in the WBZ, we exclude all crustal events. Generally speaking, crustal thickness is decreasing from north to south along the isthmus. It is about 50 km in Guatemala (Ligorría, 1995), but less than 40 km in Costa Rica (Quintero and Kulhánek,

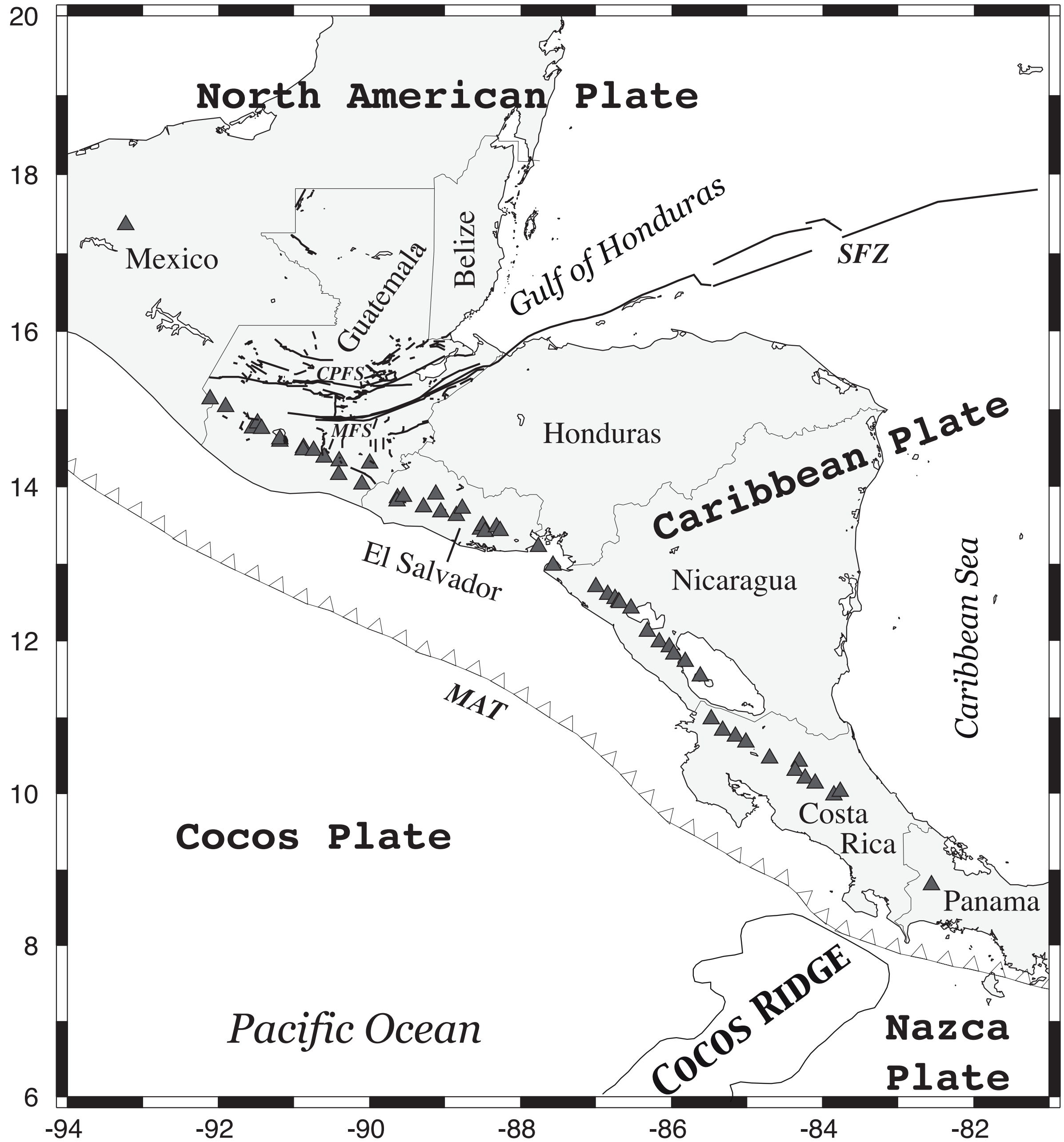

Fig. 1. Tectonic setting of Central America. Solid triangles show approximate location of volcanoes. Solid lines indicate the location of the Chixoy-Polochic fault system (CPFS) and the Motagua fault system (MFS), which continues off shore of Honduras as the Swan fracture zone (SFZ). The subduction zone boundary, i.e. the Mid-American Trench, MAT, is indicated by teeth.

1998). Consequently, only earthquakes with focal depth equal to or larger than 50 km (Guatemala, El Salvador) and 40 km (Nicaragua, Costa Rica) are included. The MIDAS catalogue was de-clustered using a script based on the algorithm of Reasenberg (1985). The script was obtained from the ZMAP software package (Wiemer and Zúñiga, 1994; Wiemer, 2001) extensively used for present calculations.

Our region of interest is exhibited in Figure 2 (areas A, B and C). It covers areas of highest seismicity comprising 2345 events and the entire Central American Volcanic Chain. After de-clustering, there are altogether 1539 events, with magnitudes that span more than four magnitude units, included in the analysis. We determined an overall *b*-value and threshold magnitude, also called the magnitude of complete-

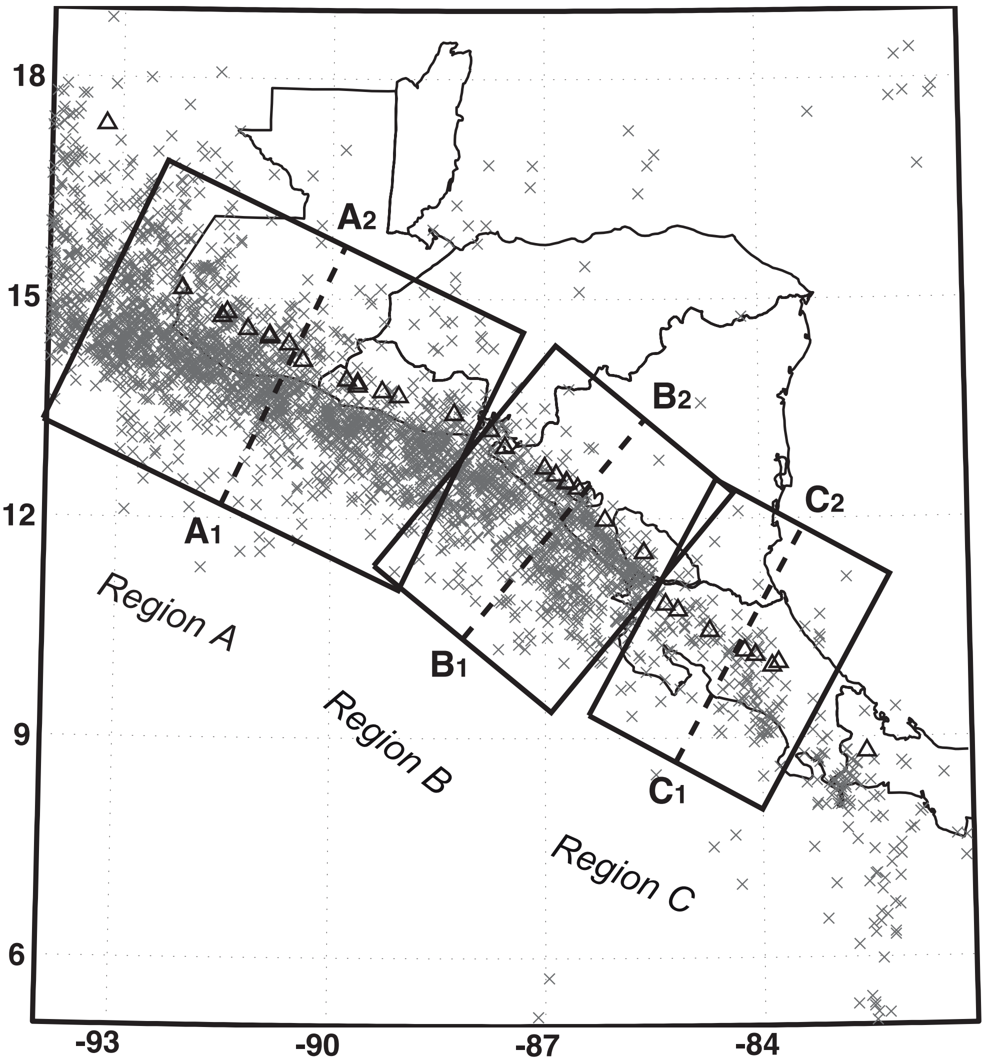

Fig. 2. Epicenters of recent (1964-1996) earthquakes (crosses) in Central America as reported by the MIDAS catalogue (M≥4, h≥40 km). Solid rectangles indicate the study regions A, B and C. Locations of cross-sections A_1A_2, B_1B_2 and C_1C_2 used in the analysis are also shown. Triangles show approximate location of volcanoes.

ness "M_c" as a function of depth and time. The b-value is calculated by applying the maximum likelihood and least-squares methods. Both approaches provide comparable results. M_c's are estimated by making use of the maximum of the derivative of FMD, which provides an overall M_c=4.2. The least-squares method gives a b-value of 0.94±0.06. The de-clustering process did not show any significant effect either on the b-value or on M_c. To examine the temporal data stability, we separated the original data into two sub-sets for periods 1964-1976 and 1976-1994. This separation was governed by a change in the gradient of the cumulative number of events observed at around 1976. b-values change from 1.16±0.08 to 0.82±0.05, respectively, while M_c decreases from 4.2 to 3.5 for the later time interval. The decrease of M_c most likely indicates an improving detection level. In later years, another change in the gradient can be spotted at around 1991. We again form two sub-intervals for the periods 1985-1991 and 1991-1994.5. b values change now from 0.90±0.05 to 0.92±0.06, respectively. FDMs for regions A, B and C are exhibited in Figure 3. As follows from the figure, the three regions provide the same threshold magnitude M_c=4.2. Dividing the entire data set into two depth ranges, i.e. 40 km 100 km and 100 km-150 km, gives M_c=4.0 for the upper slice and 4.2 for the lower slice. We concluded that the overall data sets for region A, B and C should be considered with M_c of 4.2 to ensure a stable M_c both in time and space. Consequently, throughout the present analysis we make use of a threshold magnitude of 4.2.

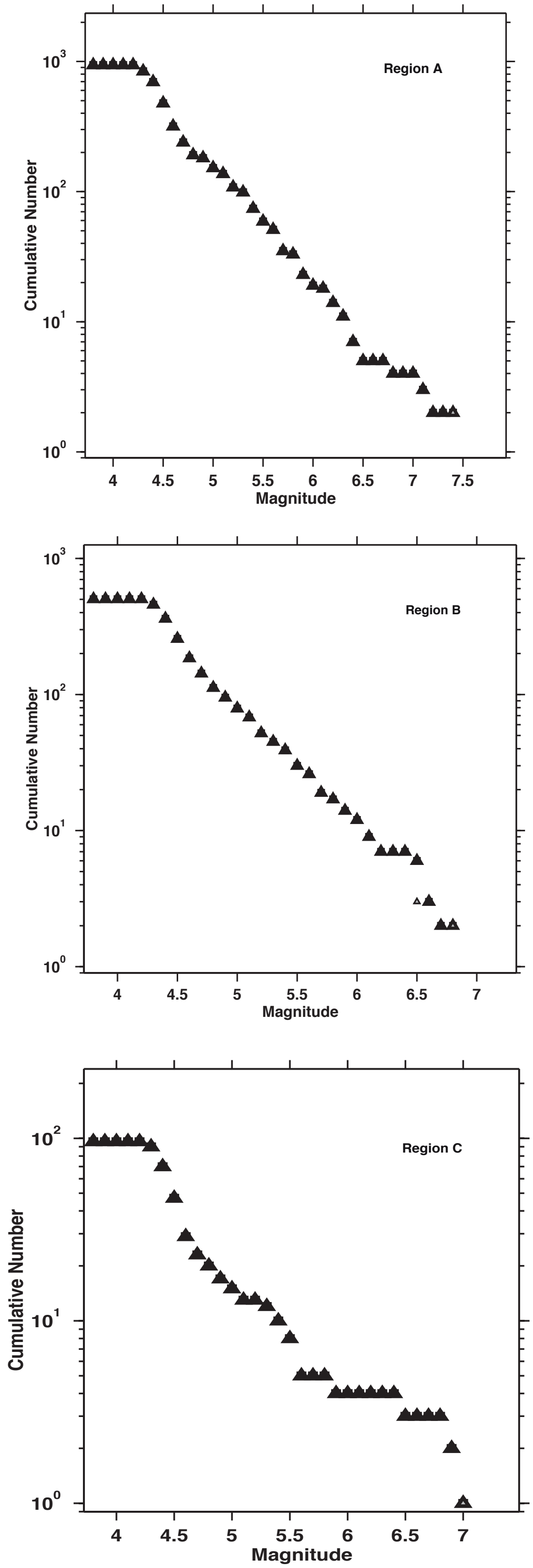

Fig. 3. Frequency-magnitude distribution for regions A, B and C. Earthquake data taken from the de-clustered MIDAS catalogue.

We cannot estimate the accuracy of magnitude reports and of hypocentral locations listed in the catalogues. However, taking into account that the region is well covered by nearby as well as distant seismographic stations and by employing two different catalogues, we believe that magnitude and/or location uncertainties are not generating the observed anomalous *b*-values. The cumulative numbers of events as a function of time, displayed in Figure 4, show no drastic changes in reporting rates, suggesting consistent observatory operations during the period under review.

Our analysis starts with generation of three sub-catalogues with epicenters inside the three rectangular regions, A, B and C (Figure 2). The overlap of regions A and B shows approximately the area where the volcano chain axis changes. The overlap of regions B and C indicates roughly the area where an offset of the volcano axis takes place.

To analyze the distribution of *b* versus depth, one-dimensional (depth slice analysis) and two-dimensional (cross-section analysis) methods were used. In both cases a sliding spatial window technique was applied. Two-dimensional mapping reveals more detail in the *b*-value distribution and is therefore superior to the one-dimensional approach, provided that the database available contains enough events. A direct comparison of results from the two approaches may, however, be difficult since the latter samples regions of high and low *b* values and necessarily provides, for a certain depth, a smoothed *b*-value of different populations. Therefore, while individual volumes of anomalous *b* may exist, it may be difficult to detect them when only the one-dimensional technique is applied. However, for data sets with a limited number of events the one-dimensional approach still may provide new information.

One-dimensional approach. We calculated *b*-values independently for each of the studied regions in vertically sliding windows (horizontal slices) containing a constant number *n* of earthquakes in the slab. We keep *"n"* constant to ensure that the change of the number of events in each window does not affect the analysis. The window, which coincides with borders of regions A, B or C, is moved downwards by 10% increments of event counts. This means that for each step, the *n*/10 shallowest events in the window are discarded and *n*/10 deeper (new) shocks are included. While *b*-value is calculated as a function of depth (i.e. the focal depth of the central event in each particular window), the time limits (i.e. 1964-1994.5) remain unchanged. The choice of the sliding-window width (number of events in each window) is a compromise between the depth resolution and the smoothing effect of broad windows. After a number of tests we used windows with 100 (area A), 75 (area B) and 40 (area C) events, with corresponding increments of 10, 7 and 4 events, respectively.

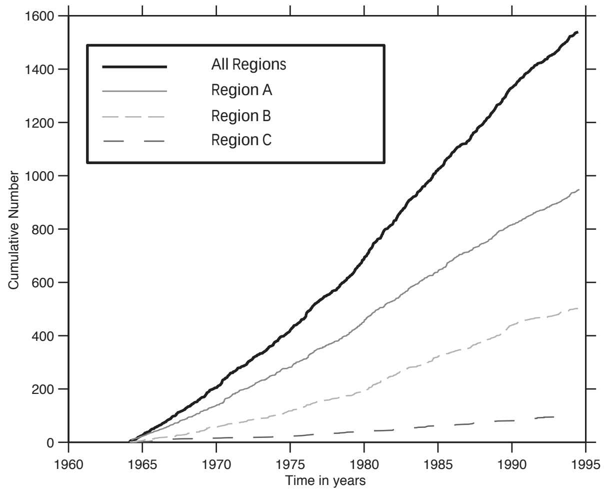

Fig. 4. Cumulative numbers of earthquakes as a function of time for the de-clustered MIDAS catalogue. From top to bottom: the whole studied region; region A; region B; region C. M_c=4.2 for all regions.

Two-dimensional approach. To envisage also the lateral (distance from the trench) distribution of *b*, we projected all hypocenters onto vertical planes perpendicular to the strike of MAT. Earthquakes in regions A, B and C were projected onto planes A_1A_2, B_1B_2 and C_1C_2, respectively (Figure 2). Vertical planes A_1A_2 and B_1B_2 were sub-divided into a 10 km x 10 km grid (due to lack of data, the two-dimensional technique could not be applied in region C). *b*-values were calculated for cylindrical volumes centered at the lower-right corner (node) of each grid element. Radii of the cylinders vary along the grid in order to contain the prescribed constant number of events, which again is a compromise between resolution and smoothing between grid nodes. After a series of tests, we chose cylinder radii comprising 100 earthquakes. To measure the resolution in our analysis, we map the radii of each cylinder in the grid (Figure 5). As follows from Figure 5, resolution becomes poor (large radii) at larger depths due to the decreasing number of events within the slab. On the other hand, for shallower depths, say, down to approximately 150 km, high resolution marks well the geometry of the WBZ. After several tests with smaller and larger radii, we decided to ignore grid sections for which the radii were larger than 60 km. This means that we limit our investigation to depths less than about 200 km for region A and less than about 220 km for region B (Figure 7).

RESULTS AND DISCUSSION

For region A, we are left with 940 events in the sub-catalogue, after de-clustering. Using a sliding window with 100 earthquakes we calculated (least-squares) an overall *b*-value of 0.94±0.06. The maximum likelihood method gives a *b*-value of 0.99±0.03. The one dimensional analysis provides the distribution of *b* with depth exhibited in Figure 6. With the least-squares method, the largest *b*-value of 1.24±0.12 is determined from a 10 km wide window centered at 78 km depth. Two local peaks can also be seen in the depth rage between 60 and 70 km. We varied the width of the window from 50 to 150 events to verify the stability of the *b*-value anomaly.

The two-dimensional analysis was performed by applying both the least-squares approximation and the maximum likelihood method. Again, the two approaches provide similar results. After data reduction due to the accepted resolution constraint, the analysis for region A comprised 779 events. The cross-section view along the profile A_1A_2 (Figure 2) is displayed in Figure 7. As follows from the Figure, the profile A_1A_2 shows two regions of higher *b* in a depth range from about 50 km to 150 km. One at a depth between 50 and 90 km in the lower part of the WBZ and the other, less distinct, at depths around 100 km in the upper part of the slab beneath the volcanic chain (marked 1 in Figure 7). To demonstrate that the latter positive anomaly in *b* is significant, we also calculated FMD for a volume centered at low *b*-value region (marked 2 in Figure 7). FMDs for the high and low *b*-value regions are significantly different at the 99% confidence level (F-test). The distributions are displayed in Figure 7. They are different within the whole magnitude range considered and follow the linear Gutenberg-Richter formula.

For region B, the sub-catalogue comprises 503 events after de-clustering. The overall *b*-value is 0.96±0.05, for the least-squares method and 0.99±0.04 for the maximum likelihood method. Considering only events within the acceptable resolution area (Figure 5), we are left with 386 events. The *b*-value as a function of depth for region B is displayed in Figure 6. There is one distinct broad maximum at a depth around 120 km. A peak value of *b*=1.34±0.13, calculated with the least-squares approximation, is obtained from a 40 km wide window centered at 124 km depth. The maximum likelihood method and the least-squares approximation show almost identical results. Sliding windows containing 75 events and focal depths equal to or larger than 40 km were used. The B_1B_2 profile reveals a dominant high *b*-value region, extending from a depth of 50 km to about 160 km at the bottom of the WBZ. A second, less distinct, positive anomaly can be seen (Figure 7) in the upper part of the slab, beneath the volcanic chain, at depths of 130-170 km. Scarcity of data in region B did not allow to perform a test of statistical significance for the latter anomaly.

For region C, only 96 events were left for the analysis. The overall *b*-value is 0.70±0.10, for the least-squares method and 0.92±0.10 for the maximum likelihood method. An attempt was made to calculate the *b*-value as a function

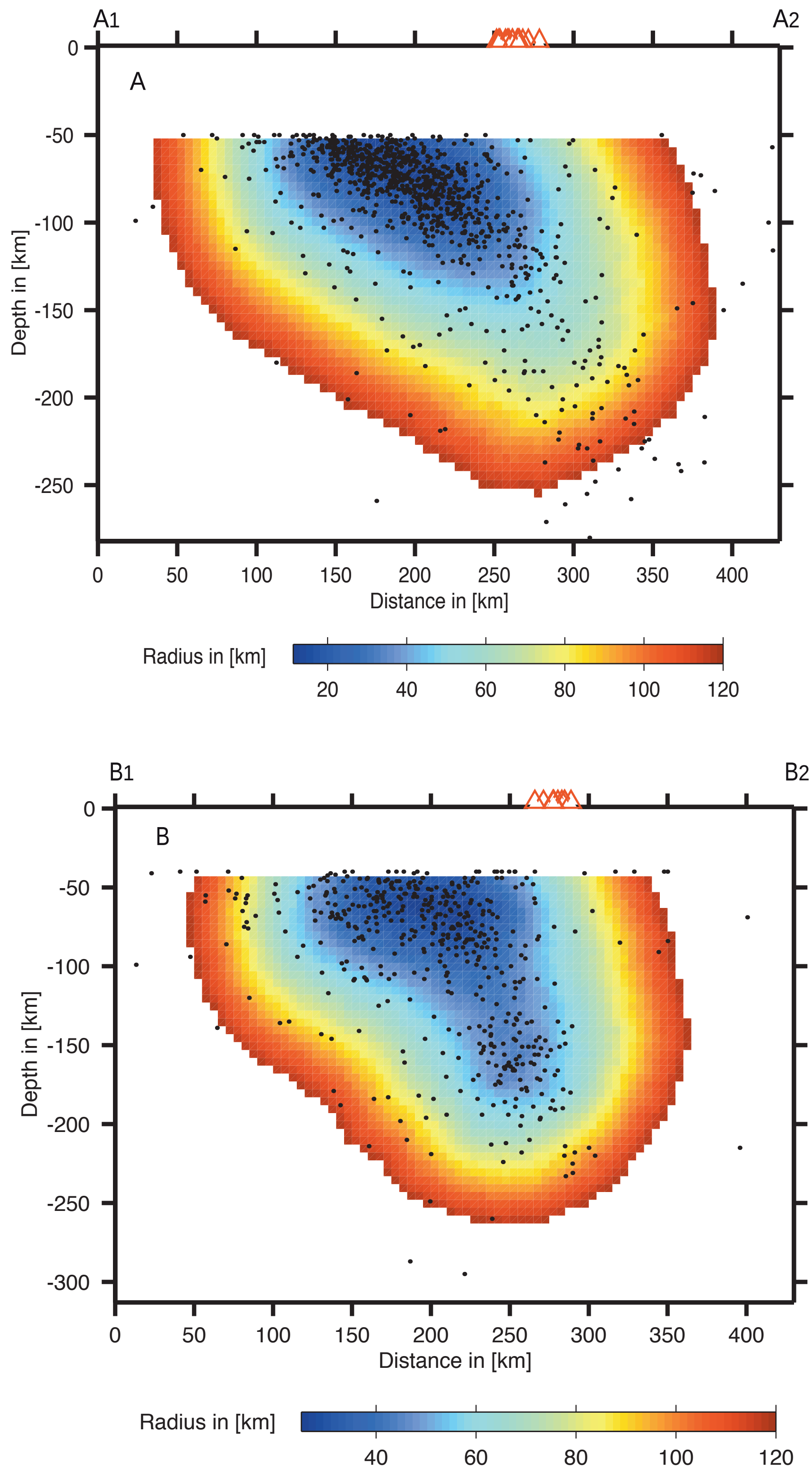

Fig. 5. Resolution maps for region A and B (MIDAS catalogue data). Red indicates low resolution. In both figures, sliding windows (cylinders) contain 100 earthquakes. Radii of sampling cylinders are plotted as function of depth and distance from the trench. The volcanic chain (red triangles) is also indicated.

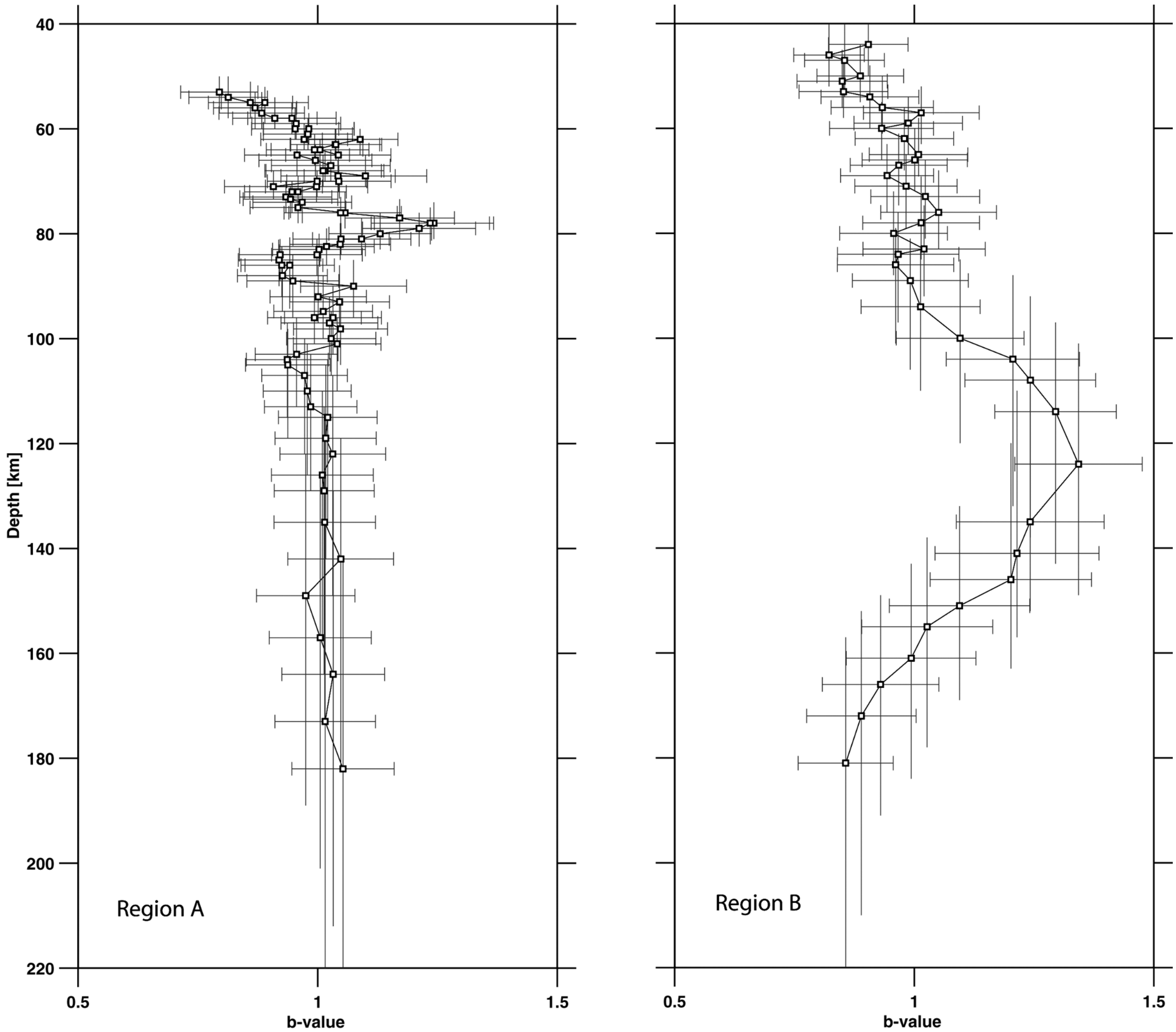

Fig. 6. *b*-value as a function of depth for region A and B using the one dimensional approach and MIDAS catalogue data. The graphs were calculated by using 100 and 75 events in the vertically sliding windows, respectively. For both regions, results calculated by maximum likelihood method are displayed. Horizontal bars indicate the standard error in the *b*-value, while vertical bars show the width of the sliding window.

of depth. Sliding windows containing 30 to 75 events were tested. We observed a broad peak in the *b* distribution at a depth of about 130 km, but due to the low number of events, we consider the results as inconclusive.

We tried to verify the obtained results by carrying out a similar analysis on another earthquake catalogue. Data sets at hand include e.g. the regional catalogue of the Central America Seismic Center, CASC. At present, information is available for the period 1992-1998 revealing Mc~4.3. However, locations and magnitude determinations listed in CASC still suffer from heterogeneous processing techniques applied by contributing national agencies leading to large errors (G. Marroquín personal communication; Ambraseys and Adams, 2001). Hence, we turned to a global catalogue of Engdahl *et al*. (1998), abbreviated to E-catalogue hereafter. The updated version provides data to 1999. The advantage of the E-catalogue is the refinement of ISC locations, in particular the focal-depth determinations (Ambraseys and Adams, 2001). Several tests show that, for Central America, the E-catalogue is complete first for magnitudes 4.8 and larger. This in turn leaves us with considerably lower number of events when compared with the MIDAS catalogue. No attempt has been made to expand the MIDAS catalogue to 1999 by adding

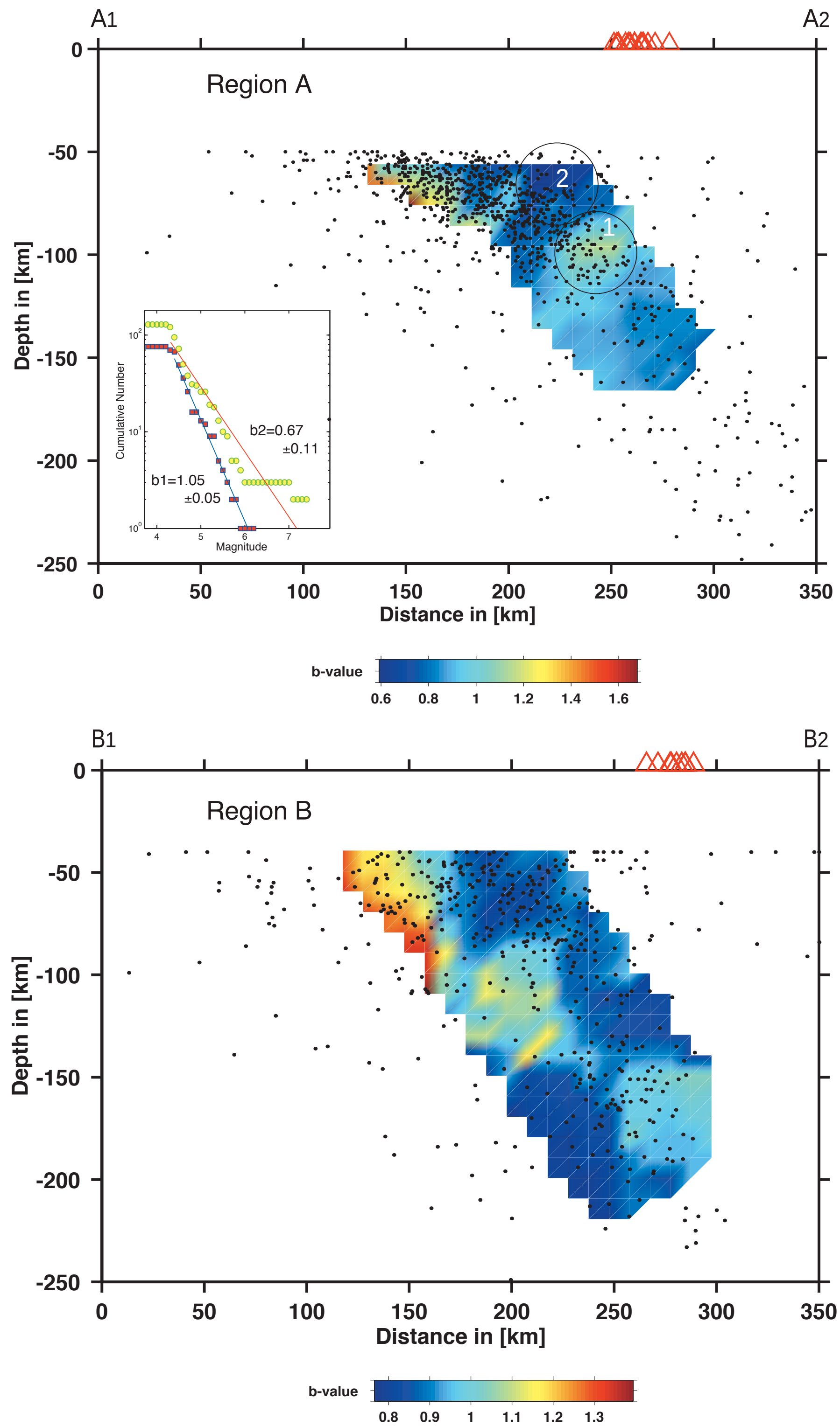

Fig. 7. Cross-sections of the *b*-value distribution (maximum likelihood, MIDAS catalogue data) along the profile A_1A_2 (upper diagrams) and B_1B_2 (lower diagrams). Blue indicates low *b*-values, whereas red shows high *b*-values. Only nodes with radii smaller than 60 km (region A) and smaller than 40 km (region B) are used. The location of the volcanic chain is also indicated. Numbered circles (upper diagram) show selected volumes of high and low *b*-values.

data from the E-catalogue due to the large discrepancy of respective threshold magnitudes.

We carried out the one-dimensional analysis on the E-catalogue for region A, making use of 595 events (M_c=4.8). Sliding windows comprising 50, 75, 100 and 150 events were examined. The *b*-value vs. depth distribution shows one peak centered at 83 km and a second broader peak centered at 95 km as determined from windows containing 100 events (Figure 8). The high *b*-values at depths around 60 km are most likely due to the relatively large volume of high *b* values in the lower part of the slab (Figure 9). The cross-section views were analyzed for radii less than 60 km comprising 75 and 100 events. The analysis with 75 events reveals high *b* values in the lower part of the WBZ at depths between 50 and 80 km and a less distinct positive anomaly in the upper part of the slab, beneath the volcanic chain, at a depth of about 100 km. These results support those obtained for region A from the MIDAS catalogue. For regions B and C, data in the E-catalogue were too scarce to carry out the analysis.

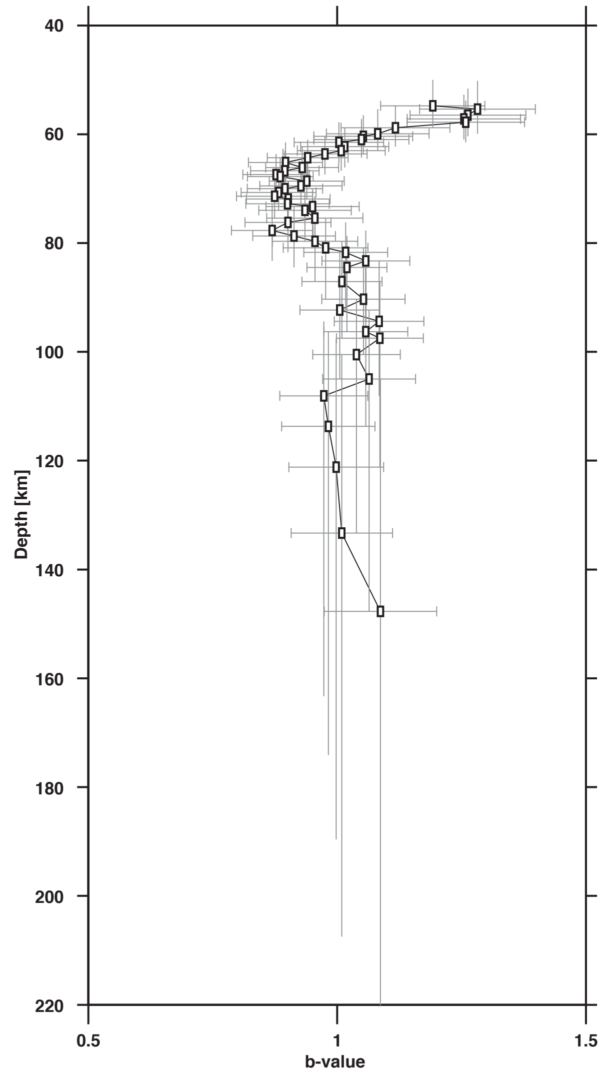

Fig. 8. *b*-value as a function of depth for region A using the one dimensional approach and data from the E-catalogue. The graph was calculated by using 100 events in the vertically sliding windows. Results calculated by maximum likelihood method are displayed. Horizontal bars indicate the standard error in the *b* value, while vertical bars show the width of the sliding window.

CONCLUSIONS

We have shown that the distribution of *b* along a large part of MAT varies significantly with depth. Our results reveal positive anomalies of *b* in the slab at depths between 50 and 170 km. A statistically significant anomaly beneath Guatemala and El Salvador, located in the upper part of the WBZ at a depth around 100 km, correlates well with results of Wiemer and Benoit (1996) concerning subduction zones of Alaska and New Zealand.

Even though the present analysis uses relatively high threshold magnitudes M_c implying low resolution, the observed anomalies are not likely to be due to our choice of input parameters. On the other hand, available earthquake catalogue data do not allow drawing a conclusive, definite description of physical processes generating the observed anomalies. We propose that the physics behind the high *b*-values could be related to thermally generated stress fields and/or to magma genesis processes taking place beneath the volcanic chain.

There is much uncertainty about the thermal structure of the descending slab. The work of Warren and Latham (1970) supports the hypothesis that regions with high *b*, such as the ones we observed in the lower part of the WBZ, may be generated by high thermal gradients. Warren and Latham (1970) conducted laboratory tests with various materials, which were exposed to large thermal gradients. They observed that thermally induced microshocks are characterized by high *b*-values in the range from 1.2 to 2.7. The subducting slab is heated by conduction (among other factors) from the surrounding hotter mantle. Large thermal gradients exist between the slab and the mantle, especially at shallower depths, say, less than 100 km. Hence the large thermal gradients could create a stress field with associated seismicity characterized by high *b*.

The high *b*-values in the upper part of the slab beneath the volcanic chain at depths around 80 and 100 km for region A, and around 150 km for region B, may be related to the magma genesis process beneath the volcanic chain. As noted by Gill (1981), *b*-values vary as a function of depth in subduction zones, which may indicate a phase transforma-

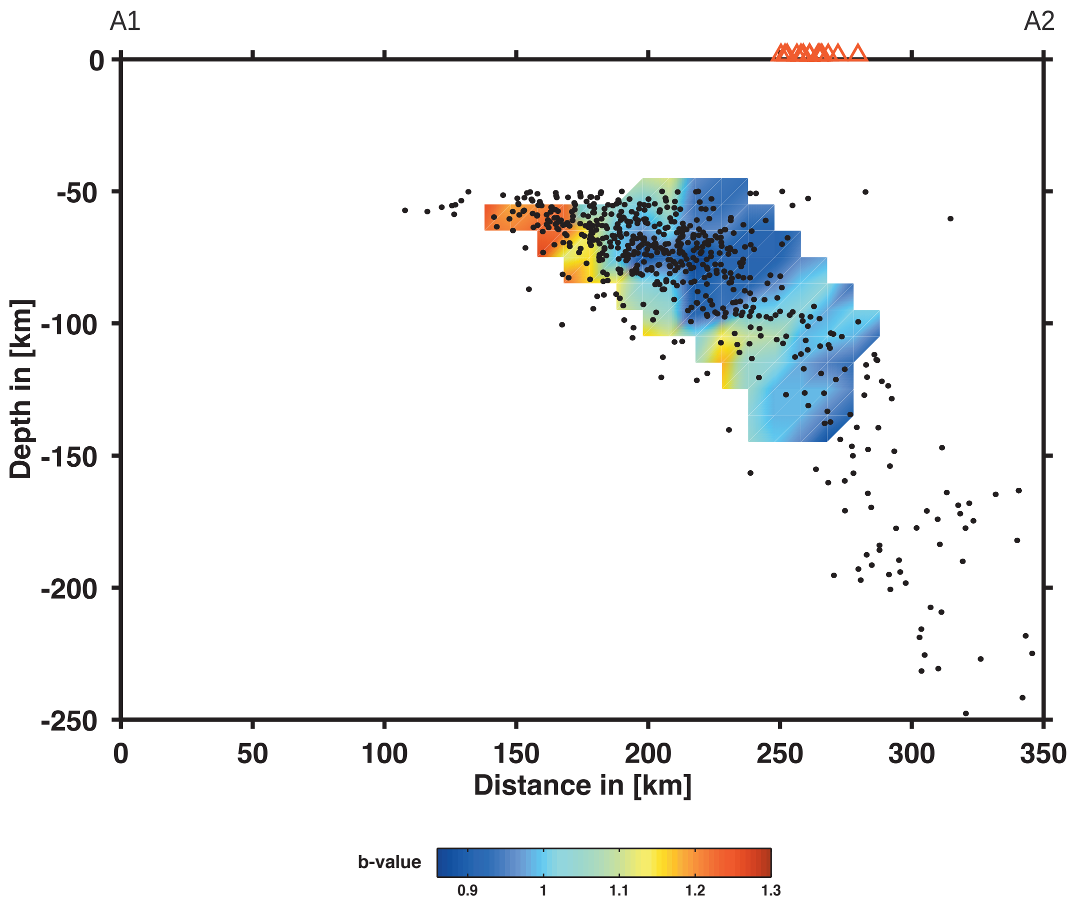

Fig. 9. Cross-section of the *b*-value distribution (maximum likelihood) along the profile A_1A_2. Data used are from the E-catalogue. Only nodes with radii smaller than 60 km are considered. Blue indicates low *b*-values, whereas red shows high *b*-values. The location of the volcanic chain is also indicated.

tion of material in the subducting slab. An increase in the *b*-value would be identifiable because the region of transformation is characterized by low stress due to high pore pressure, which results from dehydration (Anderson, 1980). Tatsumi (1986) presented a model for the volcanic front formation. He describes the process as resulting from pressure dependent reactions, ruling out the dependence upon temperature and other properties of the WBZ. According to Tatsumi (1986), the depth to the slab below volcanic chains is 112±19 km while Gill (1981) gives a depth of 124±34 km. Davies and Stevenson (1992) noted that the depth of the WBZ below volcanic chains is dependent on the dip angle, and increases for larger dip angles. In the present work, we found anomalous high *b*-values, in the upper part of the WBZ, at depths from 80 to 110 km for region A and around 150 km for region B. These results are in good agreement with depths suggested by other workers. Steeper subduction expected in region B may explain the greater depth of *b* anomalies in this section of the Cocos plate.

ACKNOWLEDGEMENTS

This work has been carried out at the Department of Earth Sciences, Seismology, Uppsala University. The Swedish Agency for Research and Educational Cooperation (SAREC) supported the work through the project Seismotectonic Regionalization of Central America (SERCA). We wish to acknowledge valuable advice and suggestions which improved the text, provided by S. Wiemer. Our thanks go to F. Guendel, E. Malavassi and A. J. Anderson for useful discussions. We appreciate constructive comments from an anonymous reviewer, which improved the presentation.

BIBLIOGRAPHY

AMBRASEYS, N. and R. ADAMS, 2001. The Seismicity of Central America. A descriptive catalogue 1898-1995, Imperial College Press, U.K., 309 pp.

ANDERSON, R., 1980, Phase changes and the frequency-magnitude distribution in the upper plane of the deep seismic zone beneath Tohoku, Japan. *J. Geophys. Res., 85,* 1389-1398.

AYELE, A. and O. KULHÁNEK, 1997. Spatial and temporal variations of seismicity in the horn of Africa from 1960 to 1993. *Geophys. J. Int., 130,* 805-810.

DAVIES, J. and D. J. STEVENSON, 1992. Physical model of source region of subduction zone volcanics. *J. Geophys. Res., 97,* 2037-2070.

ENGDAHL, E. R., VAN DER HILST and R. BULAND, 1998. Global teleseismic earthquake relocation with improved travel times, and procedures from depth determination. *Bull. Seismol. Soc. Am., 88,* 722-743.

GERSTENBERGER, M., S. WIEMER and D. GIARDINI, 2001. A systematic test of the hypothesis that the b-value varies with depth in California. *Geophys. Res. Let., 28,* 57-60.

GIBOWITZ, S. J., 1974. Frequency-magnitude depth and time relations for earthquakes in Island Arc: North Island, New Zealand. *Tectonophysics, 23,* 283-297.

GILL, J., 1981. Orogenic Andesites and Plate Tectonics, Springer-Verlag, New York, 390pp.

GUTENBERG, B. and C. RICHTER, 1954. Seismicity of the Earth and Associated Phenomena, Princeton Univ., 273 pp.

GÜENDEL, F. and M. PROTTI, 1998. Sismicidad y sismotectónica de América Central, *Física de la Tierra, 10,* 19-51.

KAGAN, Y., 1999. The universality of the frequency-magnitde relationship. *Pure and Appl. Geophys., 155,* 537-574.

LIGORRÍA, J. P., 1995. Some Aspects of Seismic Hazard Assessment in Guatemala. M.Sc. Thesis, Institute of Solid Earth Physics, University of Bergen, Norway.

LI QUAN-LIN, CHEN GIN-TIAO, YU LU and HAO BOI-LIN, 1978. Time and space scaning of the *b*-value. A method for monitoring the development of catastrophic earthquakes, *Acta Geophys. Sinica, 21,* 101-125.

MOGI, K., 1962. Magnitude-frequency relationship for elastic shocks accompanying fractures of various materials and some related problems in earthquakes. *Bull. Earthquake Res. Inst. Univ. Tokyo, 40,* 831-883.

MONTERROSO, D., 1999. Temporal and depth dependence of b-value in Central America: Application to the Motagua Fault and the subduction zone. M.Sc. Thesis, Department of Earth Sciences, Uppsala University, Sweden.

PROTTI, M., F. GÜENDEL and K. McNALLY, 1994. The geometry of the Wadati-Benioff zone under southern Central America and its tectonic significance: results from a high-resolution local seismographic network. *Phys. Earth Planet. Inter., 84,* 271-287.

QUINTERO, R. and O. KULHÁNEK, 1998. Pn-wave observations in Costa Rica. *Geofís. Inter., 37,* 171-182.

REASENBERG, P., 1985. Second order moment of Central California seismicity, 1969-1982. *J. Geophys. Res., 90,* 5479-5495.

SCHOLZ, C. H., 1968. The frequency-magnitude relation of microfracturing in rock and its relation to earthquakes. *Bull. Seismol. Soc. Am., 58,* 399-415.

TANNER, J. G. and J. B. SHEPHERD, 1997. Project Catalogue and Seismic Hazard Maps, Seismic Hazard in Latin America and the Caribbean. Pan-American Institute of Geography and History, Vol. 1, 143 pp.

TATSUMI, Y., 1986, Formation of the volcanic front in subduction zones. *Geophys. Res. Let., 13,* 717-720.

WARREN, N. W. and G. V. LATHAM, 1970. An experiment study of thermal induced microfacturing and its relation to volcanic seismicity. *J. Geophys. Res., 75,* 4455-4464.

WHITE, R., 1991. Tectonic implications of upper-crustal seismicity in Central America. *In:* Slemmons, D., Engdahl, R., Zoback, M., and Blackwell, D., (Eds), Neotectonics of North America: Boulder, Colorado, Geological Society of America, Decade Map Volume 1.

WIEMER, S., 1996. ZMAP Users Guide, 117 pp.

WIEMER, S. and J. BENOIT, 1996. Mapping the *b*-value anomaly at 100 km depth in the Alaska and New Zealand subduction zones. *Geophys. Res. Let., 23,* 1557-1560.

WIEMER, S., S. R. MCNUTT and M. WYSS, 1998. Temporal and three-dimensional spatial analyses of the frequency-magnitude distribution near Long Valley Caldera, California. *Geophys. J. Int., 134,* 409-421.

WIEMER, S. and R. ZÚÑIGA, 1994. ZMAP, a software package to analyze seismicity (abstract), EOS, Trans., AGU, 75, 456.

WIEMER, S., 2001. A software package to analyze seismicity: ZMAP, SRL, 72, 373-382.

WYSS, M., 1973. Towards a physical understanding of the earthquake frequency distribution. *Geophys. J. R. astr. Soc., 31,* 341-359.

David A. Monterroso and Ota Kulhánek

Department of Earth Sciences, Uppsala University, Villavägen 16, Uppsala S-75236, Sweden.
Email: david.monterroso@geo.uu.se
ota.kulhanek@seismo.uu.se